

Crystallization-Induced Microdomain Coalescence in Lamellar Diblock Copolymers Studied by Dynamic Monte Carlo Simulations

Wenbing Hu*

Department of Polymer Science and Engineering, State Key Laboratory of Coordination Chemistry, College of Chemistry and Chemical Engineering, Nanjing University, 210093 Nanjing, China

Received December 2, 2004; Revised Manuscript Received March 6, 2005

ABSTRACT: A numerical study of microdomain coalescence induced by the soft-confined crystallization of lamellar diblock copolymers has been reported. It was found that under high temperatures those crystallites showing their orientational preferences perpendicular to the lamellar microdomains are responsible for the occurrence of coalescence, whereas the segregation strength just plays a subsidiary role. In addition, the lamellar microdomains are well preserved with undulations at the stage of primary crystallization but be broken out by the crystal thickening at the subsequent stage of isothermal annealing. Down with the temperature, there exists an abrupt transition from perpendicular to random in the preference of crystallite orientations. Annealing the nascent crystals of variable orientational preferences demonstrates that at low temperatures a randomization in the crystallite orientations may prevent microdomains from coalescing. The mechanisms of undulation and coalescence were thus discussed on the basis of the microphase-interface tension enhanced by the crystal thickening.

I. Introduction

Nanoscale stable arrays can be produced in diblock copolymer liquids through microphase separations.^{1,2} The microstructure may contain uniformly lamellar, gyroidal, cylindrical, or spherical geometries, depending mainly upon the composition within diblock copolymers.³ Subsequent crystallization in one of two blocks incurs a spatial confinement from the microdomains of another block and gives rise to “structure-in-structure” morphologies.^{4–7} When the crystallization temperature of this block is lower than the glass-transition temperature of another block ($T_c < T_g$, the case of crystallization under a hard confinement), microdomains serve as a well-ordered pattern for the spatial distribution of crystallites. However, when the confinement becomes soft ($T_c > T_g$), the solidification (crystallization) may make a breakout of the confinement.^{8–15} This behavior exhibits a coalescence of microdomains and destroys the well-ordered microphase-separated pattern. Therefore, understanding the mechanism of coalescence will be of essential importance in the preparation of nanoscale arrays under such a soft confinement.

Quite a few of experiments have shown that during soft-confined crystallization the stability of the microphase-separated pattern might be related with the segregation strength.^{16,17} On the other hand, the coalescence can be avoided if crystallization happens at low temperatures by fast quenching,¹⁸ but it occurs once the crystallites are annealed for a long period at high temperatures.^{19–21} It turns out that the temperature is an essential factor in effect to the occurrence of coalescence. Also in experiments, it has been found that variable crystallization temperatures lead to changes in the preference of crystallite orientations.^{22,23} Therefore, the stability of the microphase-separated pattern might be even related with the preference of crystallite orientations.

Recently, we have studied the oriented primary crystal nucleation under a hard confinement of lamellar

diblock copolymer systems by means of dynamic Monte Carlo simulations.²⁴ We proved that at high temperatures the oriented block junction dictates the perpendicular preference of crystallite orientations, and if the block junction is broken, parallel preferences will occur in the process of crystal nucleation facilitated by the flat microphase interfaces. Going a step further, this lamellar diblock copolymer system can be applied to investigate the temperature dependence of crystallite orientations and its correlation with the occurrence of coalescence under a soft confinement.

Therefore, in this paper, we switch the confinement from hard to soft and make the above-mentioned investigation under both limits of strong and weak segregation. It will be shown that, under variable temperatures from high to low, an abrupt perpendicular-to-random transition occurs in the preference of crystallite orientations. In addition, the microdomain coalescence is motivated by the thickening of those perpendicular-oriented crystallites on isothermal annealing rather than by the earlier crystal growth. Meanwhile, the segregation strength serves as a subsidiary role in preserving microdomains. Moreover, random orientations of crystallites may facilitate the stability of microdomains at low temperatures. In the following text, after an introduction of simulation techniques and sample preparation, we will show the above results in company with discussions. In the end, we provide a summary of our conclusions.

II. Simulation Techniques and Sample Preparation

Like in previous dynamic Monte Carlo simulations,²⁴ polymer chains were “living” in the cubic lattice. Their microrelaxation steps allowed a single-site monomer to jump into a vacancy neighbor, accompanied by a partial sliding diffusion along the chain if necessary, and meanwhile avoided double occupation and bond crossing.²⁵ The coordination number of this cubic lattice is $q = 26$, since the bonds may stay either on the lattice axes (six neighbors) or on the face (12 neighbors) and body

* E-mail: wbhu@nju.edu.cn.

(eight neighbors) diagonals. The sample system was constructed by 7680 chains, each containing 32 units, in a 64^3 lattice box with periodic boundary conditions. We defined the symmetrical diblock copolymers as half block of each chain crystallizable (labeled as C) and another half noncrystallizable (labeled as A). Metropolis sampling was employed with a potential energy penalty $\Delta E = (bB/E_c - pE_p/E_c - c)E_c$, where b , p , and c are the net changes in the mixing AC pairs, in the parallel C bonds, and in collinear connections of consecutive bonds along the chains, respectively. Here, B is the mixing energy exchange between two species of monomers, E_p is the potential energy penalty for losing one parallel pair of C bonds, and E_c is the potential energy penalty for one noncollinear connection of two bonds along the chain. With respect to the physical meanings, the reduced energy parameter B/E_c reflects the driving interactions for microphase separation, and the reduced energy parameter E_p/E_c corresponds to the driving interactions for crystallization, while $E_c/(k_B T)$ represents the system temperature.^{26,27}

The well-ordered lamellar microdomains have been prepared in the previous study reported in ref 24, through a spontaneous microphase separation in the sample system. To this end, we performed cooling processes from a fully disordered liquid with a fixed E_p/E_c at one and a variable B/E_c "tuning" the segregation strength. The cooling program was a stepwise increase in the reciprocal temperature, as $E_c/(k_B T)$ started from zero (infinite temperature) with a step length of 0.002 and a step period of 300 MC cycles (trial moves per chain unit). In each step, the first 100 MC cycles were discarded for equilibration, and the reported data were averaged over the remaining 200 MC cycles. During each cooling process, we monitored the microphase separation by tracing the demixing parameter that was defined as the mean fraction of neighbors occupied by A monomers around each A monomer. In the meantime, we also monitored the crystallization by tracing the crystallinity that was defined as the fraction of C bonds containing more than five parallel C neighbors. Here, we choose the number of parallel neighbors at five as a demarcation of the crystalline state of C bonds (extreme number at 24 obtained from the coordination number 26 deducted by two connected bonds along the chain) separated from their noncrystalline state (extreme number at zero) to include those poorly crystalline bonds located at the crystallite surfaces. From the cooling curves shown in Figure 1a, one can see that $B/E_c = 0.5$ has already been strong enough to make the microphase separation occur much earlier on cooling than the crystallization. We picked out the state at $E_c/(k_B T) = 0.25$ ($T = 4.0E_c/k_B$) for visual inspections. In accord with our expectations, well-ordered lamellar microdomains were produced in the sample system, as demonstrated by the snapshot shown in Figure 1b.

In the following simulations, we regarded the state of Figure 1b as the initial melt for crystallization. Since there was no spontaneous glass transition in the applied range of energy parameters and temperatures, the hard confinement of microdomains was realized by simply rejecting all the trial moves involving A monomers. In the contrary case, the soft confinement allowed all these moves involving A monomers. At the temperature of $T = 4.0E_c/k_B$, the strong-segregation limit was set with $B/E_c = 0.5$, while the weak-segregation limit was set with $B/E_c = 0.2$. These settings can be applied because

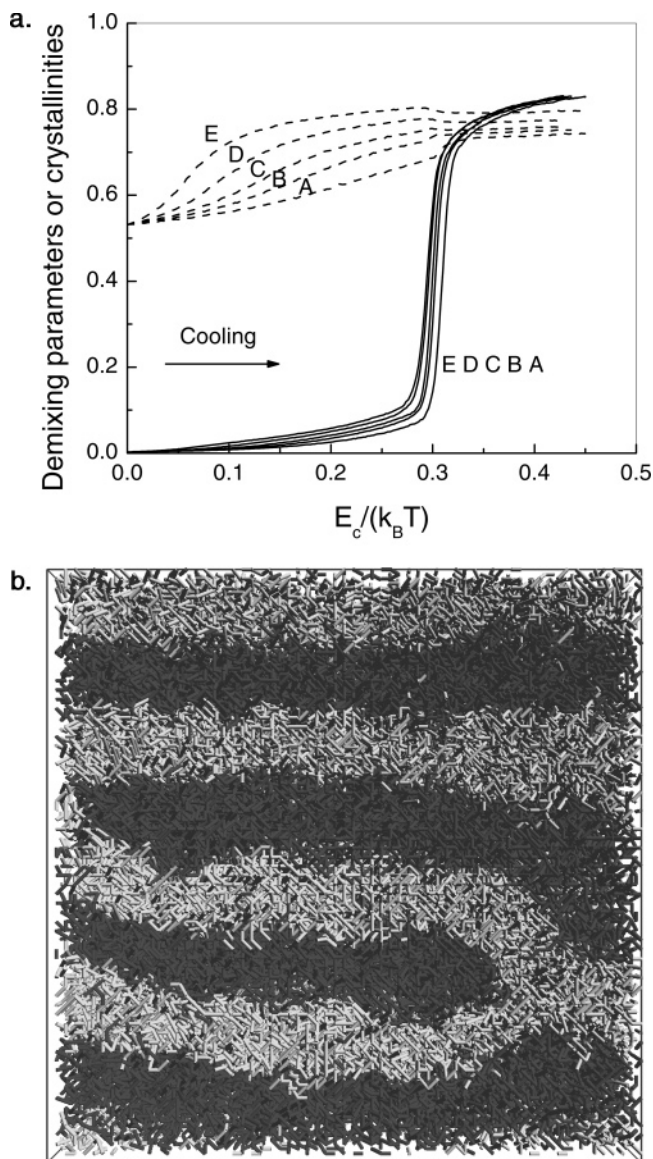


Figure 1. Preparation of lamellar microphase domains for the confined crystallization of symmetric diblock copolymers. (a) Cooling curves of demixing parameter (dashed lines) and crystallinity (solid lines) of the sample with $E_p/E_c = 1$ and variable B/E_c as 0.1, 0.15, 0.2, 0.3, and 0.5 from curve A to curve E. (b) Snapshot of the sample with $E_p/E_c = 1$ and $B/E_c = 0.5$ at the temperature of $E_c/(k_B T) = 0.25$. All the bonds are drawn in cylinders. Noncrystallizable blocks are shown in dark gray, and crystallizable blocks are in bright gray (a quotation from ref 24).

in terms of the well-known Flory–Huggins interaction parameter, the segregation strength can be estimated by $\chi N = (q - 2)B/(k_B T) \times N = (q - 2) \times B/E_c \times E_c/(k_B T) \times N = 24 \times 0.5 \times 0.25 \times 32 = 96$, close to the strong-segregation limit ($\chi N \gg 10$), and by $\chi N = 24 \times 0.2 \times 0.25 \times 32 = 38.4$, close to the weak-segregation limit ($\chi N \sim 10$).³ The cooling curves in Figure 1a show that with $B/E_c = 0.2$ the microphase separation has been finished at $E_c/(k_B T) = 0.25$; therefore, switching from the strong-segregation limit to the weak-segregation limit will not destroy the lamellar microdomains in the initial melt.

We first studied how the switching of confinement from hard to soft affected behaviors of crystallization and melting upon the temperature scanning. Then, we quenched the initial melt to the low temperatures and

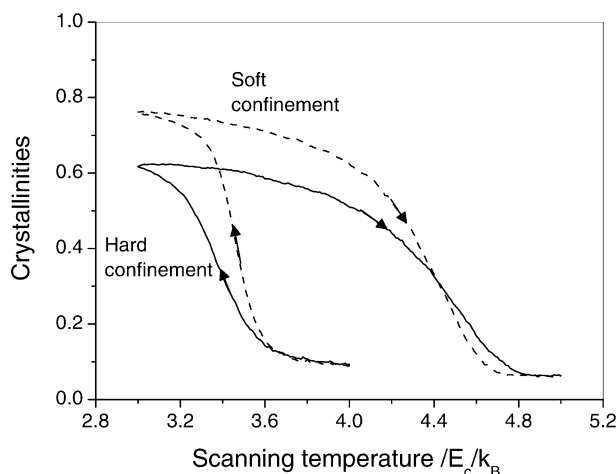


Figure 2. Cooling and heating curves of crystallinity for the initial melts of lamellar diblock copolymers under a hard confinement (solid curves) and under a soft confinement (dashed curves), both with $E_p/E_c = 1$ and $B/E_c = 0.5$. The scanning was a stepwise change in $k_B T/E_c$ with a step length of 0.01 and a step period of 100 MC cycles. The reported data were calculated at the end of each step. The arrows on the curves indicate the directions of the temperature scanning.

monitored the isothermal crystallization by tracing the time evolution of crystallinity. For the samples after the saturated crystallization, we made visual inspections on the snapshots to learn their status of coalescence. In the snapshots, the coalescence was defined as the occurrence of at least one impingements of the neighboring microdomains induced by the crystallization. We also observed their preference of crystallite orientations by calculating the orientational order parameter that was defined as

$$P = \frac{3\langle \cos^2 \theta \rangle - 1}{2} \quad (1)$$

where θ was the angle of a concerning bond referred to the direction normal to the microphase lamellae and $\langle \dots \rangle$ was an average over all the concerning bonds. Here, following the previous definition,²⁴ the concerning bonds are those C bonds containing more than 10 parallel C neighbors. According to this definition, if all the concerning bonds are normal to the microphase lamellae, P shall be equal to one; if their orientations are random, P shall close to zero; if they are all parallel to the lamellae, P approaches -0.5 .

III. Results and Discussion

Figure 2 shows two pairs of cooling and reheating crystallinity curves differing with hard and soft confinements. One can see that the softness of the crystallization environment significantly enhances both rates of crystallization and melting and makes the crystallinity approach higher. These observations are consistent with the experimental observations on cylinder-forming poly(ethylene oxide)-*b*-polystyrene (PEO-*b*-PS)/PS blends.¹⁸ Nevertheless, there appears no significant shift in the characteristic temperatures of phase transitions. On heating of the folded-chain crystallites, the melting point appears as a wide range because of a wide distribution of crystallite sizes, so the inflection points on the heating crystallinity curves represent the melting points well. On the other hand, the crystallization is initiated by

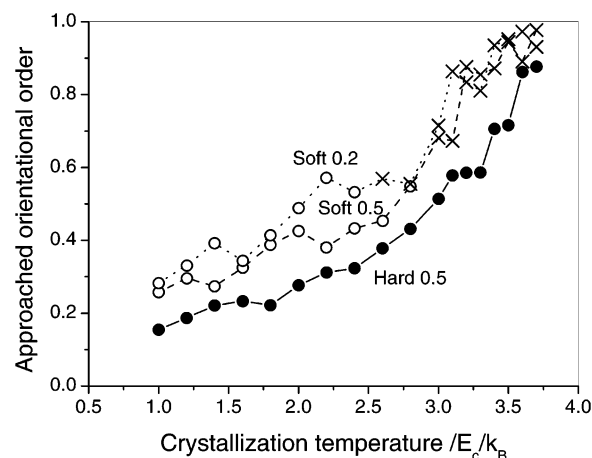


Figure 3. Approached orientational-order parameters of crystallites at variable temperatures after a saturated crystallization in the initial melt of lamellar diblock copolymers. The spheres on a solid curve are under a hard confinement with $B/E_c = 0.5$; the crosses and circles on a dashed curve are under a soft confinement with $B/E_c = 0.5$; and the crosses and circles on a dotted curve are under a soft confinement with $B/E_c = 0.2$. The status of coalescence has been marked on the curves of a soft confinement. The crosses represent for the occurrence of coalescence, and the circles mean that the lamellar microdomains are well preserved. All the isothermal processes were as long as 10 000 MC cycles for a saturated crystallization, and several cases at high temperatures were even longer. The segments are drawn to guide the eye.

crystal nucleation on cooling of the melt, and a wide temperature range for crystallization is mainly due to the kinetic delay of crystal growth upon the temperature scanning, so the onset points on the cooling crystallinity curves represent the crystallization points better than the inflection points. In Figure 2, the inflection points of both heating curves are very close, and the onset points of both cooling curves are very close, too. These observations imply that the switching of confinement mainly affects the kinetics rather than the thermodynamics of confined phase transitions.

Figure 3 compares three kinds of confinement affecting the orientational order parameters of crystallites obtained after the saturated crystallization under variable temperatures. The first one (solid line in the figure) is a hard confinement with a strong-segregation limit, the second one (dashed line) is a soft confinement still with a strong-segregation limit, and the last one (dotted line) is also a soft confinement but with a weak-segregation limit. From high to low temperatures, all the curves in the figure show a sharp jumping in the orientational-order parameters, corresponding to a transition of crystallite orientations with their preferences from perpendicular to random. In the middle temperature region, the orientational-order parameters appear quite large for showing a random preference; however, the randomness was identified by visual inspections on the snapshots, as demonstrated for example in Figure 4. The tilted preferences in crystallite orientations will make the values of orientational-order parameters in the same range, but these preferences have not been found in our visual inspections, although they were observed in experiments of PEO-*b*-PS diblock copolymers^{22,23} and they were allowed by the alignment of crystallites on the diagonal directions of cubic lattice in our simulations. So far, it is still an open question why the tilted preferences did not occur in our simulations.

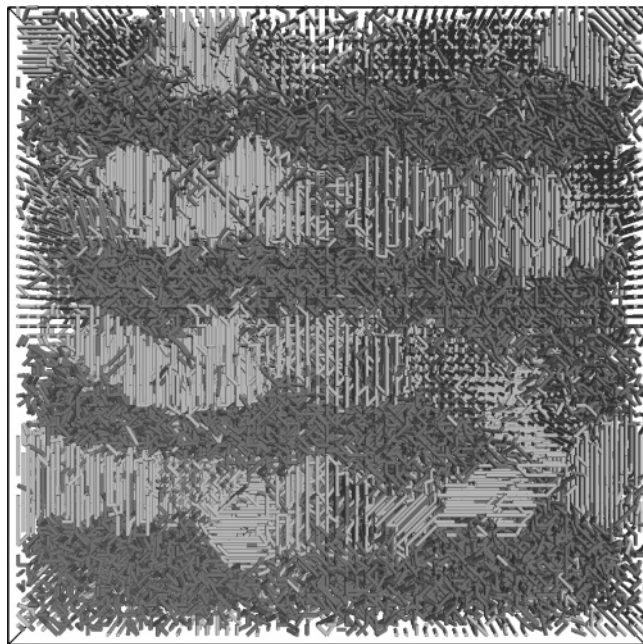


Figure 4. Snapshot of random-oriented crystallites grown and annealed at $T = 2.4E_c/k_B$ for the time period of 10 000 MC cycles in the initial melt of lamellar diblock copolymers under a soft confinement with $B/E_c = 0.5$. All the bonds are drawn in cylinders. Noncrystallizable blocks are shown in dark gray, and crystallizable blocks are in bright gray.

Figure 3 shows that the curve of the hard confinement has the highest transition temperature of crystallite orientations at $3.5E_c/k_B$, while the curve of the soft confinement with a weak-segregation limit shows the lowest one at $3.0E_c/k_B$. The randomization of crystal orientations at low temperatures can be attributed to the occurrence of primary crystal nucleation induced by other effects such as interfacial effects favoring parallel orientations, which are weaker than the effect of perpendicularly oriented block junctions at high temperatures, as explained as follows.

It is well-known that at high temperatures the rate of primary crystal nucleation is very small. A confinement in the spatial dimensions makes the event of crystal nucleation even more scarce. Nevertheless, the block junction oriented due to the microphase separation facilitates the perpendicular-oriented crystal nucleation. In addition, the flat microphase interfaces help the parallel-oriented crystal nucleation via deforming the contacted coils on the wall. When the chain length is so small as in the present simulations, the block-junction effect is dominant over all other effects at high temperatures.²⁴ Therefore, the perpendicular preference of crystallite orientations occurs at high temperatures. With the decrease of temperatures, other effects will make their contributions more significantly in the inducing of primary crystal nucleation, and ultimately, the bulk homogeneous crystal nucleation occurs. These later effects, in particular, the interfacial effects, randomize the preference of crystal orientations and give rise to an abrupt transition from perpendicular to random in the preferences of crystallite orientations. Accordingly, the transition temperature of crystal orientations is related with the conditions of microphase interfaces. Under a hard confinement, the transition from perpendicular to random occurs in priority because the solidlike interface is the most favorable condition for interfacial-induced crystal nucleation. Under a soft

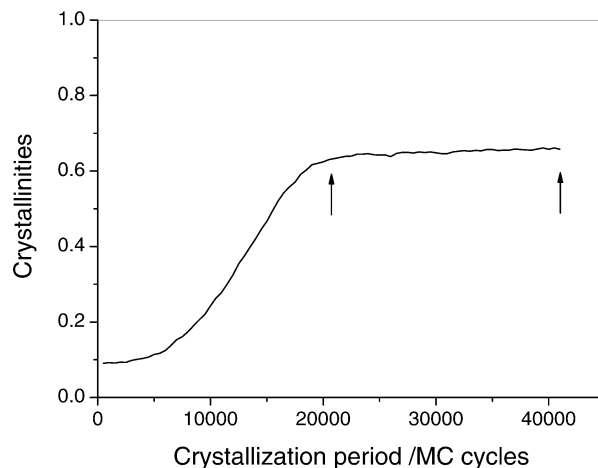


Figure 5. Isothermal evolution curve of crystallinity at $T = 3.7E_c/k_B$ for the initial melt of lamellar diblock copolymers under a soft confinement with $B/E_c = 0.2$. Two arrows indicate the time points where the snapshots are made.

confinement, the strong-segregation limit facilitates flat and sharp interfaces and hence makes a higher contribution to the parallel-oriented crystal nucleation than the weak-segregation limit. This explains the transition sequence of the crystallite orientations under three kinds of confinement observed in Figure 3.

In the middle temperature range, the events of perpendicular-oriented crystal nucleation coexist with the parallel-oriented and other-oriented nucleation events, and their contributions to the orientational-order parameter decrease with the temperature. This fact explains the behaviors of the orientational-order parameters that appear quite large for the random orientations in Figure 3 and decrease with the temperature.

After the crystallization had saturated under variable temperatures, the status of microdomain coalescence were inspected on snapshots. The results are shown also in Figure 3, with the crosses representing the occurrence of coalescence and the circles no coalescence. From this figure, one can see that with a perpendicular preference of crystallite orientations at high temperatures the coalescence occurs, whereas with random orientations of crystallites at low temperatures the lamellar microdomains can be well preserved. In addition, switching the segregation limit from strong to weak just causes a small shift of the boundary between the coalescence and the well preservation. These results imply that the temperature or the preference of crystallite orientations plays a dominant role in the occurrence of coalescence, while the segregation strength appears to play only a subsidiary role.

To our surprise, when we traced the time evolution of coalescence during isothermal crystallization at high temperatures, we found that in all cases the lamellar microdomains were well preserved at the stage of primary crystallization, and the coalescence occurs only at the subsequent stages of isothermal annealing. As an example, Figure 5 shows the time-evolution curve of crystallinity at $T = 3.7E_c/k_B$ for the initial melt under a soft confinement with the weak-segregation limit. We picked out two states from this curve for visual inspections: one located at the time point immediately after the primary crystallization and another at the time point after a long-term isothermal annealing. Their snapshots are shown in parts a and b of Figure 6, respectively. One can see that the lamellar micro-

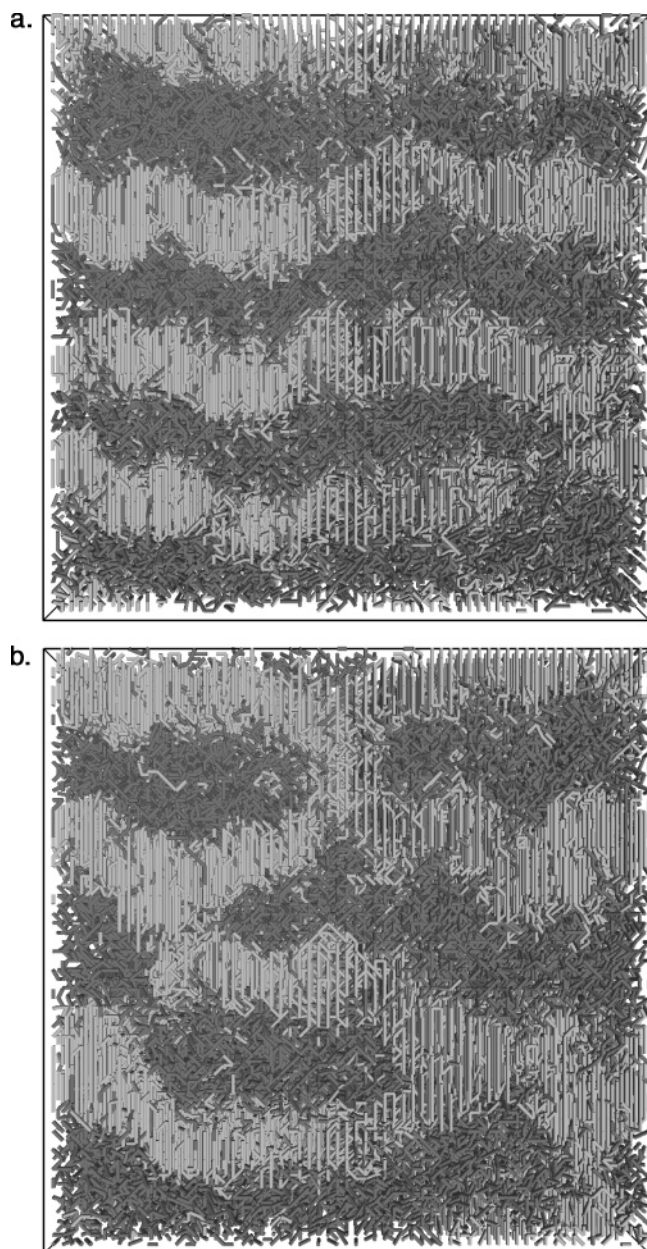


Figure 6. Snapshots of well-preserved lamellar microdomains at 21 000 MC cycles (a) and coalesced microdomains at 41 000 MC cycles (b), taken from the isothermal crystallization process shown in the preceding figure. All the bonds are drawn in cylinders. Noncrystallizable blocks are shown in dark gray, and crystallizable blocks are in bright gray.

domains are well preserved in Figure 6a, while the coalescence has already occurred in Figure 6b.

Figure 6a also demonstrates an undulation phenomenon in microphase lamellar domains as a result of crystallization under a soft confinement. This crystallization-induced undulation is consistent with recent experimental observations on PS-*b*-poly(L-lactide) diblock copolymers.²⁸

From visual inspections on snapshots like Figure 6b, we further found that the breakout of microdomains appears always as the thickening of those perpendicular-oriented crystallites followed with an impingement to the neighboring crystallites in the next microdomains. We thus concluded that the thickening of those perpendicular crystallites can be regarded as the motivation of microdomain coalescence, whereas the strength of

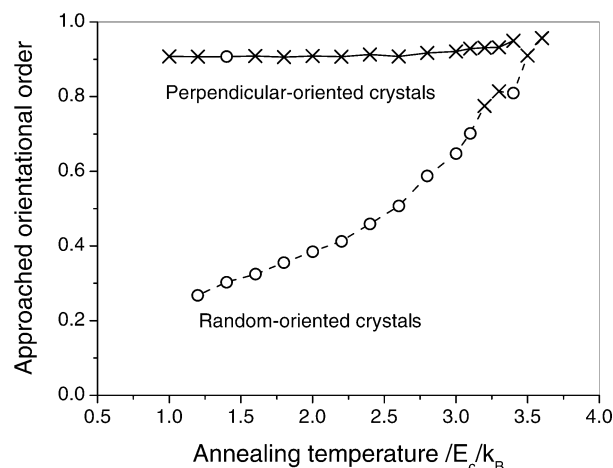


Figure 7. Status of coalescence for the perpendicular-oriented (solid curve) and the random-oriented (dashed curve) nascent crystallites, marked on the corresponding curves of orientational-order parameters vs variable annealing temperatures after annealed for 10 000 MC cycles. From the initial melt of lamellar diblock copolymers under a soft confinement with $B/E_c = 0.5$, the perpendicular-oriented sample was prepared at $T = 3.5E_c/k_B$ for 4000 MC cycles, and the random-oriented sample was prepared at $T = 1.0E_c/k_B$ for 2000 MC cycles.

segregation just plays a secondary role in preserving the microdomains by hindering the crystal thickening at the microphase boundaries.

High temperatures provide high activities of the crystal thickening; meanwhile, the perpendicular preference contains a high probability of break-out by crystal thickening. To learn which one is a more fundamental factor in giving rise to the coalescence of microdomains, we performed annealing experiments on two kinds of nascent crystals with different orientational preferences. The first one was produced at a high temperature to contain a significantly perpendicular preference of crystallite orientations, and the second one was produced at a low temperature to contain a quite random preference of crystallite orientations. According to the time-evolution curves of crystallinity in isothermal crystallization, two nascent states of crystals were picked out at the end of primary crystallization where the lamellar microdomains were well preserved. Then, they were annealed under variable temperatures for 10 000 MC cycles. The final status of coalescence and the approached orientational-order parameters are shown in Figure 7. In this figure, one can see that for the first sample the coalescence occurs over the whole temperature region of our observations, while for the second sample the coalescence occurs only in the high-temperature region, accompanied by a significant transition of crystallite orientations to the perpendicular preference. Figure 7 clearly demonstrates that to give rise to the coalescence of microdomains the perpendicular preference of crystallite orientations is a much more fundamental factor than the system temperature.

Since the snapshots provide the morphology limited on a sectional area like the thin section of a sample under the transmission electron microscopy, the status of coalescence cannot be precisely judged by the visual inspection. Accidentally, Figure 7 shows that the microdomains are preserved in the first sample at $T = 1.4E_c/k_B$ and in the second sample at $T = 3.4E_c/k_B$. They can, nevertheless, be regarded as the isolated incidences.

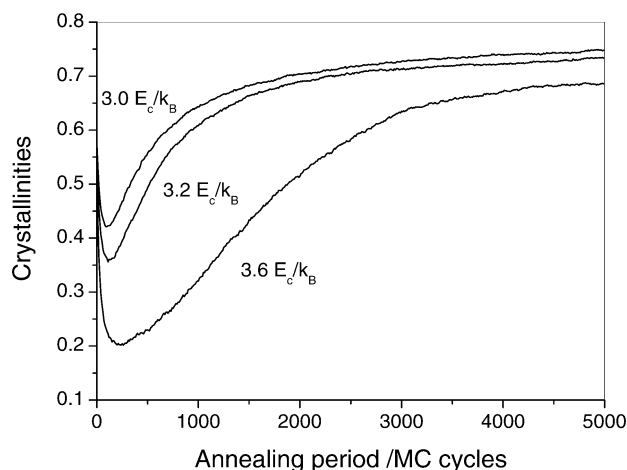


Figure 8. Time-evolution curves of crystallinity at variable annealing temperatures as indicated nearby, for the random-orientated crystallites prepared at $T = 1.0E_c/k_B$ for 2000 MC cycles in the initial melt of lamellar diblock copolymers under a soft confinement with $B/E_c = 0.5$.

On annealing the second sample at high temperatures, the time-evolution curves of crystallinity reveal a significant melting–recrystallization process for the reorganization of crystallite orientations, as demonstrated in Figure 8. The recrystallization produces a perpendicular preference of crystallite orientations that is intrinsic in the crystallization under high temperatures and hence gives rise to the coalescence of microdomains. In other words, the random orientations of crystallites may facilitate to preserve the lamellar microdomains, particularly at low temperatures without a significant recrystallization. This observation is consistent with the experiments.^{18–21} The mechanism of melting–recrystallization of polymer crystals is worth of further study in future. Here, it appears that the memory of random orientations of crystallites has been completely eliminated by the local melting, and the recrystallization is initiated by the isolated events of crystal nucleation depending only upon the temperature.

Microphase interfaces are the key to understanding the microdomain coalescence motivated by the crystal thickening. In bulk homopolymer systems, chain-folded crystals are always metastable and tend to thicken until all the chains are fully extended. However, in the lamellar diblock copolymer systems with only one block crystallizable, the fully extended chains are not the most stable state of the whole molecules on account of a strong entropy penalty on the extending of amorphous blocks. To maintain microdomains in lamellar shapes, there exists an equilibrium fold length for the crystalline block tied with the amorphous block on both sides of microphase interfaces, provided that the crystalline stems are perpendicular to the interfaces.^{29,30} Therefore, in the ideal model of lamellar microdomains, the crystal thickening will eventually stop at the equilibrium fold length rather than at the fully extended chain length. In the dilute solutions of diblock copolymers, the lamellar microstructure may be well preserved with such an equilibrium fold length in the crystallites.^{31–33} However, in the bulk phases, the crystalline blocks are always trying to make chain-extending even beyond the equilibrium fold length. The overthickening gives rise to an additional interfacial tension produced by the crowding of those amorphous blocks and hence leads to a curva-

ture of microphase interfaces. As a result, the undulation of lamellar domains occurs. This explains the previous conjecture²⁸ that the occurrence of undulation can be attributed to the interfacial stress due to crystallization. It turns out that during isothermal crystallization the primary crystallization raises the interfacial tension high enough to produce undulation but not enough to produce coalescence. Further thickening of perpendicularly oriented crystals in the subsequent stage of isothermal annealing will enhance the curvature of interfaces until the coalescence occurs. Nevertheless, parallel and tilted orientations of crystallites can efficiently decrease the surface tension produced by the crowding of those amorphous blocks. This explains why a randomization of crystallite orientations can preserve the lamellar microdomains well.

Even the confined extended-chain crystals may still have microdomain coalescence. The crystalline blocks can make the extended conformation stable by accommodating themselves in an interdigitated style, provided that the crystalline blocks have much larger sectional area than the backbone of amorphous blocks so that the entropy penalty on the extending of the latter can be efficiently released, like in the case of the rigid rod connected with a flexible tail.³⁴ Nevertheless, the interdigitated extended-chain crystals (single layer) will further thicken to the noninterdigitated extended-chain crystals (double layer). This is because if we disregard the strong entropy penalty on the extending of the amorphous blocks, the free ends of crystalline blocks will have much lower surface free energy in the double layer than in the single layer. During such crystal thickening, the surface crowding of the amorphous blocks will naturally induce microdomain coalescence.

IV. Conclusions

By means of dynamic Monte Carlo simulations, we studied the microdomain coalescence induced by the soft-confined crystallization of lamellar diblock copolymers. We found that from high to low temperatures the saturated isothermal crystallization showed a transition from perpendicular to random in the preference of crystallite orientations. During isothermal crystallization, the primary crystallization only produces undulation of lamellar domains, while the subsequent isothermal annealing, in particular, the thickening of those perpendicularly orientated crystals, makes the occurrence of coalescence. In the meantime, the segregation strength seems to play a subsidiary role in the occurrence of coalescence. Moreover, a randomization of crystallite orientations can preserve the lamellar microdomains effectively. As an explanation to the above observations, the occurrences of undulation and coalescence can be attributed to the interfacial tension of microdomains enhanced by the thickening of those perpendicularly oriented crystals.

Acknowledgment. The author thanks the reviewer for reminding him of the interdigitated extended-chain case in discussions. Part of this work was initiated during the author's stay in FOM Institute for Atomic and Molecular Physics, The Netherlands. Dawning 300A Instruments at Nanjing University have been used in computation. The funds from National Natural Science Foundation of China (NSFC Grant No. 20474027) and Nanjing University (Talent Introducing Fund No. 0205004108 and 0205004215) are appreciated, too.

References and Notes

- (1) Bates, F. S.; Fredrickson, G. H. *Annu. Rev. Phys. Chem.* **1990**, *41*, 525.
- (2) Muthukumar, M.; Ober, C. K.; Thomas, E. L. *Science* **1998**, *277*, 1225.
- (3) Hamley, I. W. *The Physics of Block Copolymers*; Oxford University Press: Oxford, 1998.
- (4) Hamley, I. W. *Adv. Polym. Sci.* **1999**, *148*, 113.
- (5) Loo, Y.-L.; Register, R. A.; Ryan, A. J. *Phys. Rev. Lett.* **2000**, *84*, 4120.
- (6) Fairclough, J. P.; Mai, S.-M.; Matsen, M. W.; Bras, W.; Messe, L.; Turner, S.; Gleeson, A. J.; Booth, C.; Hamley, I. W.; Ryan, A. J. *J. Chem. Phys.* **2001**, *114*, 5425.
- (7) Hamley, I. W.; Castelletto, V.; Floudas, G.; Schipper, F. *Macromolecules* **2002**, *35*, 8839.
- (8) Douzinas, K. C.; Cohen, R. E. *Macromolecules* **1992**, *25*, 5030.
- (9) Nojima, S.; Kato, K.; Yamamoto, S.; Ashida, T. *Macromolecules* **1992**, *25*, 2237.
- (10) Rangarajan, P.; Register, R. A.; Adamson, D. H.; Fetters, L. J.; Bras, W.; Naylor, S.; Ryan, A. J. *Macromolecules* **1995**, *28*, 1422.
- (11) Ryan, A. J.; Hamley, I. W.; Bras, W.; Bates, F. S. *Macromolecules* **1995**, *28*, 3860.
- (12) Rangarajan, P.; Register, R. A.; Fetters, L. J.; Bras, W.; Naylor, S.; Ryan, A. J. *Macromolecules* **1995**, *28*, 4932.
- (13) Hamley, I. W.; Fairclough, J. P.; Ryan, A. J.; Bates, F. S.; Towns-Andrews, E. *Polymer* **1996**, *37*, 4425.
- (14) Quiram, D. J.; Register, R. A.; Marchand, G. R.; Ryan, A. J. *Macromolecules* **1997**, *30*, 8338.
- (15) Rohadi, A.; Endo, R.; Tanimoto, S.; Sasaki, S.; Nojima, S. *Polym. J.* **2000**, *32*, 602.
- (16) Quiram, D. J.; Register, R. A.; Marchand, G. R. *Macromolecules* **1997**, *30*, 4551.
- (17) Loo, Y.-L.; Register, R. A.; Ryan, A. J. *Macromolecules* **2002**, *35*, 2365.
- (18) Hong, S.; Bushelman, A. A.; MacKnight, W. J.; Gido, S. P.; Lohse, D. J.; Fetters, L. J. *Polymer* **2001**, *42*, 5909.
- (19) Zhu, L.; Mimnaugh, B. R.; Ge, Q.; Quirk, R. P.; Cheng, S. Z. D.; Thomas, E. L.; Lotz, B.; Hsiao, B. S.; Yeh, F.; Liu, L. *Polymer* **2001**, *42*, 9121.
- (20) Huang, Y.-Y.; Chen, H.-L.; Li, H.-C.; Lin, T.-L.; Lin, J.-S. *Macromolecules* **2003**, *36*, 282.
- (21) Huang, Y.-Y.; Yang, C. H.; Chen, H.-L.; Chiu, F.-C.; Lin, T.-L.; Liou, W. *Macromolecules* **2004**, *37*, 486.
- (22) Zhu, L.; Cheng, S. Z. D.; Calhoun, B. H.; Ge, Q.; Quirk, R. P.; Thomas, E. L.; Hsiao, B. S.; Yeh, F.; Lotz, B. *J. Am. Chem. Soc.* **2000**, *122*, 5957; *Polymer* **2001**, *42*, 5829.
- (23) Huang, P.; Zhu, L.; Cheng, S. Z. D.; Ge, Q.; Quirk, R. P.; Thomas, E. L.; Lotz, B.; Hsiao, B. S.; Liu, L. Z.; Yeh, F. J. *Macromolecules* **2001**, *34*, 6649.
- (24) Hu, W.-B.; Frenkel, D. *Faraday Discuss.* **2005**, *128*, 253.
- (25) Hu, W.-B. *J. Chem. Phys.* **1998**, *109*, 3686.
- (26) Hu, W.-B. *J. Chem. Phys.* **2000**, *113*, 3901.
- (27) Hu, W.-B.; Frenkel, D.; Mathot, V. B. F. *J. Chem. Phys.* **2003**, *118*, 10343.
- (28) Ho, R. M.; Lin, F. H.; Tsai, C. C.; Lin, C. C.; Ko, B. T.; Hsiao, B. S.; Sics, I. *Macromolecules* **2004**, *37*, 5985.
- (29) DiMarzio, E. A.; Guttman, C. M.; Hoffman, J. D. *Macromolecules* **1980**, *13*, 1194.
- (30) Whitmore, M. D.; Noolandi, J. *Macromolecules* **1988**, *21*, 1482.
- (31) Lotz, B.; Kovacs, A. J. *Kolloid Z. Z. Polym.* **1966**, *209*, 97.
- (32) Lotz, B.; Kovacs, A. J.; Bassett, D. C.; Keller, A. *Kolloid Z. Z. Polym.* **1966**, *209*, 115.
- (33) Kovacs, A. J.; Lotz, B.; Keller, A. *J. Macromol. Sci. Phys. B* **1969**, *3*, 385.
- (34) Matsen, M. W.; Barret, C. *J. Chem. Phys.* **1998**, *109*, 4108.

MA047516D